581507

WHITE PAPER: SORPTION AND THE WIPP CHEMISTRY CONCEPTUAL MODEL

Patrick V. Brady, Sandia National Laboratories, 4/22/24

INTRODUCTION

The Chemistry Conceptual Model for the WIPP CCA conservatively assumed no sorption in the disposal area. The magnitude of the continuing "no sorption" conservatism is estimated here. Actinide (An) sorption to waste Fe corrosion products, waste soil and cement, and Salado fines will occur because all have high surface areas and are known to sorb Ans (Section 1). Sorption is calculated to lower dissolved An concentrations to well below An solubility limits. Sorption to MgO should also lower microbe, and possibly humic acid (HA), levels in the disposal area (Sections 2 and 3). The Appendix describes the potential impact of waste phosphate on dissolved An concentrations in the absence of sorption. All sections identify studies that would decrease uncertainty in the analysis.

The scoping calculations provide the technical basis for a closer experimental examination of sorption that might establish reduction of An mobility at WIPP. The calculations use measured or estimated sorption coefficients, assume simple mixing of disposal area fluids with average waste compositions, minor chemical communication with the Salado disturbed rock zone (DRZ), and are appropriate for a scoping analysis of sorption at WIPP.

SECTION 1. ACTINIDE SORPTION IN THE DISPOSAL AREA

The WIPP waste disposal area will contain 7.47e7 kg of Steel and Fe Metals/Alloys, some of it corroded, 7.98e6 kg of soil, and 1.52e6 kg of cement (Table 1), as well as collapsed Salado. To assess the potential importance of sorption in the disposal area, sorption partition coefficient K_ds are estimated for the selected disposal area solids. A K_d (mL/g) is the ratio of the concentration of a sorbed component (for example, in moles/g) to its dissolved concentration (for example, moles/mL). A K_d greater than zero indicates sorption; the larger the K_d, the more sorption that occurs. K_ds are specific to the conditions under which they are measured. The most predictive K_ds for the disposal area are those measured in WIPP (or WIPP-similar) brines containing sorbates below their solubility limits on minerals (so that the K_d only measures sorption, not precipitation + sorption) of similar grain size to those expected in the disposal area. K_ds measured in WIPP brines are better than K_ds measured in seawater which are themselves better than K_ds measured in dilute solutions. To be predictive, K_ds should be measured on the grain size of the solid of interest: for example, a K_d measured on fine sand will be much larger than a K_d measured on gravel because of the sand's higher specific surface area. All K_ds below are for solids that are expected to have high specific surface areas (≥ 5 M^2/g) in the disposal area, the exception being MgO which has a lower surface area of 0.4 M^2/g.

WIPP:4.4.2.2.1:PA:QA-L:574933

Information Only

1 of 30

Table 1. Waste and Packaging Materials[a].

Waste Materials	CH Mass (kg)	RH Mass (kg)	Total (kg)
Iron-based Metal/Alloys	1.98E+07	9.70E+05	**2.08E+07**
Aluminum-based Metal/Alloys	4.56E+05	9.24E+04	5.48E+05
Other Metal/Alloys	1.15E+06	1.54E+05	1.30E+06
Other Inorganic Materials	1.17E+07	9.41E+05	1.26E+07
Cellulose	4.13E+06	2.10E+05	4.34E+06
Rubber	1.16E+06	5.29E+04	1.21E+06
Plastic	5.70E+06	3.13E+05	6.01E+06
Cement	1.51E+06	2.89E+03	**1.51E+06**
Solidified Inorganic Material	1.24E+07	5.03E+04	1.25E+07
Solidified Organic Material	3.88E+06	1.32E+04	3.89E+06
Soil	7.97E+06	1.15E+04	**7.98E+06**
Vitrified	--	--	--
Packaging Materials			--
Cellulose	2.58E+06	--	2.58E+06
Plastic	3.68E+06	9.42E+05	4.62E+06
Rubber	9.92E+04	5.20E+03	1.04E+05
Steel	3.92E+07	1.47E+07	**5.39E+07**
Lead	--	1.04E+07	1.04E+07
Grand Total	1.15E+08	2.89E+07	1.44E+08

[a]From Table 5-5 of Van Soest (2022). Fourth column added. Focus of the present analysis bolded.

Corrosion products, soil, and cement (and the Salado) are focused on here because reasonable estimates can be made of their An K_ds and surface areas. Together they make up 58 % of the waste and packaging material mass. Other high mass categories (> 10^6 kg) include, in order of mass: Other Inorganic Material, Solidified Inorganic Material, Plastic, Lead, Cellulose, Solidified Organic Material, Other Metal/Alloys, and Rubber. These make up the rest of the waste.

There will be more surface sites in the disposal area than Am + Th + Pu in the WIPP inventory. The WIPP Am and Th inventories (calculated from Reed, 2015) are expected to be 835 and 5.9e4 moles. The Pu inventory (including surplus Pu) is expected to be 2.1e5 moles (calculated from Figure S-1, National Academies Press, 2020). Assuming a default surface site density of 2.3 surface sites/nm^2 (Davis and Kent, 1990) of disposal area solids, means that WIPP Am + Th + Pu would occupy 7.2e10 m^2 of disposal area surface. While the surface area of the collapsed Salado available for sorption is impossible to estimate accurately, there will be an estimated maximum of 1.74e12 m^2 of Fe corrosion products, 8.0e11 m^2 of soil, and 1.5e11 m^2 of cement alone in the disposal area (calculated by multiplying the mass of each by an assumed surface area – see below), suggesting an abundance of surface sites for Ans to potentially sorb to.

Information Only

To sorb to disposal area surface sites, Ans must displace more abundant Na and Mg. Experimental evidence for An displacement of Na and Mg is discussed below. Lastly, over-pressurizing of the disposal area post-closure should favor exposure of solid surfaces.

Estimation of K_ds

Fe Corrosion Products

Low carbon steel corrosion at WIPP is likely to produce corrosion products of magnetite, green rust – a ferrous hydroxide solid solution, and hibbingite (Wang et al., 2001; Nemer et al., 2011). The An(III)-corrosion product K_d is set to 10^6 mL/g from Morelova's (2020, Figure 56B) measurement of uptake of 5.1e-10 M of the Am analogue Eu by magnetite in 4.7 M NaCl at pH 8. Under the same conditions, the hibbingite Eu K_d was ~ $10^{5.7}$ mL/g. Because of near-complete Eu sorption, most of Morelova's (2020) K_ds were measured near or below the detection limit of dissolved Eu. Sorption was largely independent of NaCl.

Since the disposal area will have Mg levels of 0.4 – 0.8 M (Domski, 2023), many disposal area surface sites should be occupied by Mg, in addition to Na. But Mg at WIPP levels may not have a large impact on Eu sorption to Fe corrosion products as Morelova (2020, Figure A61) observed pH 8, Eu = 5.1e-10 M, sorption to magnetite in 0.96 M NaCl and 0.95 M $MgCl_2$ solutions to be the same, suggesting no specific Mg competition, though any competition might have been obscured by measurements being at or below the Eu detection limit. Morelova (2020, Figure 71) did see a substantial effect of Mg on Eu = 5.1e-10 M sorption to hibbingite at pH > 8, albeit in higher Mg solutions than the WIPP disposal area brines. Luckscheiter and Kienzler (2001) found Th sorption to corroded nuclear waste glass in 5.5 M NaCl and 5.0 M $MgCl_2$ brines to be "very similar" at 80°C and pH 6.5. An(III), or An(III) analogue, K_d measurements in WIPP brine would be a useful way to incorporate any Mg effect in the sorption model.

Because no measurements of Th sorption by Fe corrosion products in WIPP-like brine can be found in the literature, the An(IV) – Fe corrosion product K_d in the disposal area is assumed to be that of Th in seawater measured on SiO_2, $CaCO_3$, Fe_2O_3, Al_2O_3, and TiO_2; ~ 10^5 ml/g (Lin et al., 2015, Table 1). The fact that all the minerals sorbed Th suggests that Fe corrosion products will sorb An(IV) as well. Seawater has a marginally lower pH, and 10x lower ionic strength, and lower Mg, than disposal area brine will. In the absence of WIPP-specific measurements, sorption measurements done in seawater are assumed to apply to disposal area brine. An(IV) K_d measurements on WIPP corrosion products in WIPP brine would be better.

The hibbingite surface area is assumed to be 13.1 m^2/g, the magnetite surface area measured by Morelova (2020), in the absence of published hibbingite measurements.

Information Only

Soil and Cement

Baes and Sharp (1983) gave geometric mean soil Th and Am K_ds of 6e4 and 1800 mL/g for pH 4.5 – 9.0 solutions. Ochs et al. (2016) gave best estimate Th and Am K_ds of 3e4 and 1e4 mL/g for sorption onto degraded cement ("State 4"). K_d measurements made on both in WIPP brine would be better.

The surface area of soil is assumed to be 100 m^2/g. Soil surface areas vary widely, between < 0.1 (clean sand) and 800 m^2/g (montmorillonite clay). A surface area of 100 m^2/g would be typical of a soil made up of 12.5 % montmorillonite clay.

The surface area of cement is assumed to be 100 m^2/g. Thomas et al.'s (1999) review indicated cement paste surface areas of 80 – 280 m^2/g. Grambow et al. (2020) measured cement paste surface areas of 8 – 50 m^2/g.

Salado Fines

Dosch and Lynch (1978) measured Pu(IV) K_ds of 17 – 59 mL/g on Salado halite + clay, and a Pu(IV) K_d of 6700 mL/g on Salado anhydrite alone. Dosch and Lynch (1978) measured Am K_ds of 11 – 306 mL/g on Salado halite + clay, and an Am K_d of 290 mL/g on Salado anhydrite alone (Carlsen and Platz (1986) also documented sorption of Am by halite and anhydrite from non-WIPP solutions). Dosch and Lynch's (1978) measurements were done from pH 6.5 – 8.4. Dosch and Lynch (1978) identified clay as the most important An-sorbing mineral in the Salado. In the calculations below, Dosch and Lynch's (1978) measured average K_ds are raised to levels expected for 1% clay, the presumed clay content of the Salado, using Dosch and Lynch's (1978) clay-only K_d measurements (Dosch and Lynch's (1978) experiments were done with Salado containing 0.17% and 0.28% clay, and no anhydrite). Because the disposal area Salado is 10% anhydrite, the K_ds must be raised as well using the anhydrite-only K_d measurements of Dosch and Lynch (1978). The calculated K_ds for Am and Pu(IV) on Salado containing 1% clay, 10% anhydrite, and 89% halite are 949 mL/g (Am) and 825 mL/g (Pu(IV)). The K_ds are mass-weighted sums of the K_ds on clay and anhydrite; halite is assumed to have a K_d of 0 ml/g for all Ans.

These K_ds would only apply to small grain sizes such as used in Dosch and Lynch's (1978) experiments. These are referred to as "Salado fines" below. Larger grain sizes, which would make up the vast bulk of the collapsed Salado in the disposal area would have much lower surface areas, and much lower K_ds. Dosch and Lynch (1978) measured their sieved < 74 micron material to have surface areas of ~ 5 m^2/g. High surface area Salado clays (44.6 m^2/g – Park et al., 1995) will be preferentially exposed in the disposal area because the Salado separates at the clay and anhydrite layers when it collapses (DOE, 2013; MSHA, 2016). Clay occurs in the

Information Only

repository horizon "as discrete layers from less than one to a few centimeters thick; finely disseminated clays are also dispersed uniformly through the halite" (Krumhansl et al., 1990).

Sorption vs. Solubility in the Disposal Area

An sorption in the disposal area is calculated as a mass-weighted sum of sorption to Fe corrosion products (cp), soil, cement (cem), and Salado fines:

$$An_{sorbed}/An_{dissolved} = X_{cp} \bullet K_{d,An\text{-}cp} \bullet C_{cp} + K_{d,An\text{-}soil} \bullet C_{soil} + K_{d,An\text{-}cem} \bullet C_{cem} + X_{fines} \bullet K_{d,An\text{-}fines} \bullet C_{fines}$$

An_{sorbed} and $An_{dissolved}$ are the amount of An sorbed and dissolved (mol/L), and C is the grams of the particular subscripted material in the disposal area (g/ml, calculated from Table 2). K_ds are listed in Table 2. $X_{Fe\text{-}cp}$ is the mole fraction of Fe that has converted to hibbingite before a DBR, assumed here to be 0.5. X_{fines} is the fraction of Salado exposed to a DBR that will be fines in the disposal area, assumed here to be 0.01.

Table 2. Parameters for An Sorption to Fe Corrosion Products, Salado Fines, Cement, Soil, and MgO.

Sorption	K_d (mL/g)	Mass (g)	Surface area (m^2/g)
An(III) to Fe corrosion products	1e6	1.32e11[a]	13.1[b]
An(IV) to Fe corrosion products	1e5		
An(III) to Salado fines	949	6.92e12[c]	5 (Fines)[d]
An(IV) to Salado fines	825		
An(III) to Cement	1e4	1.51e9[e]	100
An(IV) to Cement	300		
An(III) to Soil	810	7.98e9[e]	100
An(IV) to Soil	6e4		
Humic Acids to MgO	28.6	2.70e10[f]	0.4[g]
Microbes to MgO	18 - 45		

[a]Hibbingite, calculated from PAIR Fe-Alloy + Steel masses (Table 1). [b]Assumed to be the same as Morelova's (2020) magnetite surface area. [c]Calculated from DRZ volume of King (2021), 3.07e6 M^3 divided by the density of the Salado, 2.25 g/ml; this is the <u>total</u> mass in the repository Salado DRZ, of which fines adjacent to the waste will be a small, unknown fraction. [d]From Dosch and Lynch (1978). [e]from Table 1 (PAIR). [f]Calculated from Domski (2023) analysis assuming half of MgO converted to hydromagnesite (Domski, 2023). [g]Approximately 50% of the WIPP MgO sieves to < 0.75 microns and has a B.E.T.-measured surface area of 0.575 m^2/g (10/30/23 emails to the author from Melissa Mills). The 50% that sieves above 75 microns will have a surface area greater than 0 m^2/g, but less than 0.575 m^2/g. So 0.225 m^2/g was assumed for the > 75 micron fraction to give an overall WIPP MgO surface area of 0.4 m^2/g.

Information Only

Table 3 shows predicted An levels after dissolving the WIPP inventory of Am, Pu (50% Pu(III): 50% Pu(IV)), and Th into the minimum DBR volume and allowing it to sorb to the selected disposal area solids. The last two columns compare An levels predicted by sorption control and solubility control, the present WIPP approach. The first three columns show the relative impact of disposal area sorbents; corrosion products > soil + cement > Salado fines. The calculations assume the presence of sorbents and that disposal area fluids and sorbents will be well-mixed.

Table 3. Sorption vs. Solubility Prediction of Dissolved An Levels (M)

	Sorption Soil + cement	**Sorption** Soil + cement + 1 % Salado fines	**Sorption** Soil + cement + 1 % Salado fines + 50 % Fe corrosion	**Solubility**[a]
Th	1.1E-07	1.0E-07	8.2E-09	5.3E-08
Pu(III)	4.9E-06	1.2E-06	1.6E-09	3.4E-06
Pu(IV)	2.0E-07	1.8E-07	1.5E-08	5.3E-08
Am	3.9E-08	9.6E-09	1.3E-11	3.4E-06

[a]From King (2023), for GWB, includes 4.2e-5 M EDTA (see below).

Effects of Organic Ligands

An uncertainty in the calculation is any effect of organic ligands on An K_ds as organic ligand complexation of Ans can decrease An K_ds. Organic ligand effects are not included in the calculation above. EDTA is emphasized here because it raises WIPP An(III) solubility by a factor of 11 - 13 in the minimum direct brine release volume (Domski, 2023); EDTA complexation of An(IV) is much less significant (Domski, 2023). The other organic ligands - acetate, oxalate, and citrate - form weaker complexes with Ans and are susceptible to biodegradation by halophiles under WIPP conditions (Swanson et al., 2013).

WIPP presently assumes an inventory-limited EDTA concentration of 4.2e-5 M in the minimum DBR volume (Domski, 2023). This number over-estimates EDTA mobilization of An(III) because it conservatively ignores EDTA biodegradation + sorption before disposal and biodegradation + sorption once disposed but before anoxic conditions prevail at WIPP.

<u>EDTA Biodegradation</u>

EDTA is biodegraded under oxidizing conditions, but not under anoxic conditions such as will prevail at WIPP after ~ 100 years. EDTA in WIPP waste will have seen over a hundred years of non-anoxic conditions (above + below ground) before the disposal area goes anoxic and EDTA biodegradation ceases. EDTA in waste soil, e.g. from INEEL Pit 9 (Cantrell and Riley, 2008), will have seen decades of soil-like conditions (soil was used as a backfill at Pit 9) before disposal at WIPP. Biodegradation is therefore likely to have reduced EDTA levels before disposal. The same should be true for other soil-associated EDTA bound for WIPP.

Information Only

EPA assigns EDTA a biodegradation half-life of "weeks to months" (https://www.federalregister.gov/documents/2006/03/08/06-2106/ethylenediaminetetraacetic-acid-chemicals-exemptions-from-the-requirement-of-a-tolerance). Means et al. (1980) measured biodegradation and chemical degradation + sorption + photolysis of 2e-3 M EDTA in respectively biologically active and sterile soil microcosms for 173 days. In the absence of biodegradation (chemical degradation + sorption only) EDTA levels had decreased 28 % in 173 days. Photolysis + chemical degradation + sorption decreased EDTA levels by 39 % over 173 days. Biodegradation decreased EDTA levels by 86.7 – 98.4 % over 173 days. The EDTA biodegradation half-life in the no-nutrient-added microcosm was ~ 60 days. Nutrient-added biodegradation half-lives were ~ 10 – 20 days. Wen et al. (2009) measured 14 % EDTA degradation in 20 days in Cd and Zn contaminated soil, but 30 % EDTA degradation in 20 days in uncontaminated soil. Guo et al. (2015) measured soil EDTA half-lives of 21 – 75 days. An EDTA soil half-life of 2 – 3 months for soil-associated EDTA in WIPP waste would be consistent with the measurements cited above and EPA guidance.

EDTA Sorption

EDTA sorbs to cement (Nalet and Nonat, 2016; Maragkou and Pashilidis, 2021), to magnetite (Blesa et al., 1984), and as EDTA or EDTA complexes to soils, sediments, and other oxide minerals (Serne et al., 1996). Byegard et al. (1999) measured substantial sorption of REE-EDTA complexes, analogues to An(III)-$EDTA^-$, to crushed granite, including clays, from a high salinity solution.

Impact of EDTA

The work of Seliman et al. (2010) is used to roughly estimate the impact of EDTA on WIPP disposal area sorption of An(III). Seliman et al. (2010) measured Am K_ds on a soil from the Inshas low-level waste disposal site, Arab Republic of Egypt, as a function of EDTA to be: K_d = 1.8e4 mL/g (EDTA = 0), K_d = 2300 mL/g (EDTA = 1e-6 M), K_d = 1600 mL/g (EDTA = 1e-5 M), and K_d = 290 mL/g (EDTA = 1e-4 M). These values suggest a K_d of ~ 1300 ml/g at 4.22e-5 M EDTA, the WIPP inventory-limited value, i.e. an 11.4 - fold decrease in the Am K_d from the "no EDTA" case.

The work of Hakem et al. (2001) is used to estimate the impact of EDTA on WIPP disposal area sorption of An(IV): Hakem et al. (2001) measured Pu(IV) uptake on Hanford soil from distilled water held to pH 5.25. Hakem et al.'s (2001) measured Pu(IV) as a function of dissolved EDTA/Pu(IV) would predict a decrease in Pu(IV) sorption by ~ 30 % relative to the "no EDTA" case if the presumed WIPP EDTA/Th ratio in Domski (2023) were used.

Information Only

Table 4 shows the effect of decreasing all model An(III) K_ds by a factor of 11.4, from the analysis of the work of Seliman et al. (2010), and increasing final An(IV) concentrations by 30 %, from the analysis of the work of Hakem et al. (2001) (who did not report their data as K_ds). An levels in Table 3 increase 10 – 30 % from the baseline "no EDTA" case, but are still lower than WIPP-predicted solubilities. Because of EDTA biodegradation + sorption the effect of EDTA on sorption-controlled An levels would be less than that shown in Table 3. The calculation assumes that the EDTA effect on sorption measured by Seliman et al. (2010) and Hakem et al. (2001) would be similar at WIPP.

Table 4. Effect of EDTA on Sorption.

	Sorption Soil + cement + 1 % Salado fines + 50 % Fe corrosion No EDTA	Sorption Soil + cement + 1 % Salado fines + 50 % Fe corrosion, 4.2e-5 M EDTA	Solubility[a] 4.2e-5 M EDTA
Th	8.2E-09	1.1E-08	5.3E-08
Pu(III)	1.6E-09	1.8E-08	3.4E-06
Pu(IV)	1.5E-08	1.9E-08	5.3E-08
Am	1.3E-11	1.4E-10	3.4E-06

[a]From King (2023), for GWB.

The key point from Table 4 is that ignoring sorption is conservative for An(III)s and An(IV)s. Solubility calculations exceed sorption-limited concentrations of Th by a factor of 5, Pu(III) by a factor of 200, Pu(IV) by a factor of ~ 3, and Am by more than 4 orders of magnitude. This would make the formation of An solubility-limiting phases unlikely. The sorption-limited values in Table 4 would be lower still if more Fe corrosion were assumed, if corrosion products from rock bolts and wire mesh had been included in the calculation, and if Pu sorption to MgO (Farr et al., 2000, 2007) had been included.

Waste Heterogeneity

An important use of the sorption model is to quantify the intrinsic sorptive capacity of WIPP waste at a room, or waste package, level and to determine if heterogeneous An inventories will ever exceed it.

The most heterogenous An inventory is likely CH-waste that will contain ~ 300 g (1.25 moles/bbl) of Surplus Pu compared to non-Surplus Pu CH-waste packages which contain ~ 14 g Pu on average (NAS, 2020). The rest of the package will include adulterant, a polyethylene liner, possibly a lead and/or polyethylene shield insert, but mostly plywood/fiberboard dunnage (e.g. Reedlunn and Bean, 2019, Figure 1.1), wood held together by urea-formaldehyde glue.

The potential for steel corrosion products and degraded dunnage to sorptively limit Pu release from Surplus Pu CH-waste is substantial. There will be an estimated 1.65 moles (maximum) of hibbingite surface sites, and an estimated 11.6 moles of dunnage surface sites in a fully

Information Only

corroded/degraded drum. The surface of undegraded wood has 0.11 moles of carboxylate + phenolate groups per kg wood (Tiruta-Barna and Schiopu, 2011).

HA sites are apparently preserved during biodegradation; from Berl and Koerber (1938) "Anaerobic and aerobic bacteria which decompose cellulose do not attack cellulose humic acids, lignin, and lignin humic acids at all." The present analysis therefore assumes wood carboxylate + phenolate groups will be preserved through biodegradation. HA release from degraded dunnage at WIPP would be limited by HA's low solubility in WIPP brine, 2 mg/L.

Pu sorption in a Surplus Pu CH-waste package is estimated as a mass-weighted sum of sorption to Fe corrosion products and biodegraded dunnage (Salado fines were found to have a minimal effect and were left out of the calculation):

$$Pu_{sorbed}/Pu_{dissolved} = X_{cp} \bullet K_{d,An\text{-}cp} \bullet C_{cp} + K_{d,An\text{-}dunnage} \bullet C_{dunnage}$$

In the calculation, X_{cp} was assumed, as above, to be 0.5; 50% of the steel was assumed to be converted to corrosion products. C_{cp} was calculated from the steel inventory in the PAIR (Van Soest, 2022) to be 2.06 g/ml. $C_{dunnage}$, 6.72 g/ml, was calculated assuming 150 liters of biodegraded dunnage in a 55 gallon (208 L) barrel, having a density of 0.7 kg/L. The Pu(III) and Pu(IV) corrosion product K_ds, $K_{d,An\text{-}cp}$, were the same ones used above, respectively 10^6 ml/g and 10^5 ml/g. In the absence of WIPP-specific measurements of Pu(III) sorption to humic-rich organic material, the $K_{d,An(III)\text{-}dunnage}$, was set to 1.12e5 ml/g, the Am K_d recommended by Thibault et al. (1990) for organic soils. The $K_{d,An(IV)\text{-}dunnage}$, was set to 1.75e5 ml/g, Lin et al.'s (2015) measured seawater Th-HA K_d, 7.94e6 ml/g, lowered by a factor 45.5 to convert HA carboxylate + phenolate to wood carboxylate + phenolate sites. The conversion is the average number of carboxylate + phenolate sites in 4 HAs measured by Marquardt et al. (2004, Table 1), 5 mol/kg, divided by the number of carboxylate + phenolate sites on wood, 0.11 mol/kg (Tiruta-Barna and Schiopu, 2011). The average HA site densities of Marquardt et al. (2004) were used because Lin et al. (2015) did not report their HA site density.

Sorption inside the Surplus Pu CH-waste packages is calculated to limit Pu(IV) to 1.6e-8 M and Pu(III) to 1.2e-8 M, respectively, a factor of 3 and 200 lower than solubility-predicted levels. Again, the sorption-limited values would be lower still if more Fe corrosion were assumed, if corrosion products from rock bolts and wire mesh had been included in the calculation, if corrosion products from the stainless steel sleeve holding the Pu + adulterant had been included, and if Pu sorption to MgO (Farr et al., 2000, 2007) had been included. In short, waste sorption might limit dissolved An concentrations for the most extreme inventory heterogeneity, Surplus Pu.

To decrease uncertainty, $K_{d,An(III)\text{-}cp}$, $K_{d,An(IV)\text{-}cp}$, $K_{d,An(III)\text{-}dunnage}$ and $K_{d,An(IV)\text{-}dunnage}$ might be measured in WIPP brine at high An loadings, the distinguishing feature of the Surplus Pu packages. The K_d approach is less certain at high surface loading. For the dunnage K_d measurements, the sorbent should be anaerobically degraded plywood/fiberboard. The technical literature on anaerobic

Information Only

biodegradation of wood might be examined more closely to quantify resistance of HAs to biodegradation.

Other Waste Sorbents

Again, 41 % of the waste will consist of Other Inorganic Material, Solidified Inorganic Material, Plastic, Lead, Cellulose, Solidified Organic Material, Other Metal/Alloys, and Rubber. They were not included in the calculation above because many of the wastes are likely to be heterogeneous, particularly Other Inorganic Material, Other Metal/Alloys, and Solidified Organic Material, making their sorptive properties hard to estimate without examining the WIPP waste inventory more closely. But the fact that Ans sorb to some extent to most inorganic and organic surfaces would make such an effort useful. Doing so would only increase the calculated An uptake by disposal area solids.

WIPP conservatively assumes complete conversion of Cellulose, Plastic, and Rubber to CO_2 at present. Pb at WIPP is expected to corrode to hydrocerussite, $2PbCO_3 \cdot Pb(OH)_2$, for which no An sorption data can be found. Because the WIPP Pb inventory will be large, it would be useful to determine An-hydrocerussite K_ds under WIPP conditions.

Uncertainty Reduction

To decrease uncertainty the following analyses might be done, listed in presumed order of importance:

1. Measure the An(III) and An(IV) K_ds for hibbingite (and/or magnetite and green rust) under WIPP conditions at low and high surface loadings, and corrosion product surface areas measured from WIPP steel corrosion experiments,

2. Measure An(III) and An(IV) K_ds for anaerobically degraded dunnage under WIPP conditions at high surface loadings,

3. Estimate bounding K_ds and surface areas for Other Inorganic Material, Solidified Inorganic Material, Plastic, Lead, Cellulose, Solidified Organic Material, and Other Metal/Alloys, if possible.

4. Measure An-hydrocerussite K_ds in WIPP brine, and

5. Examine the setting and history of the individual WIPP EDTA waste streams to estimate the extent of EDTA breakdown + sorption, above and below ground, before a DBR. The aim would be to estimate how much waste EDTA is soil-associated (or otherwise biodegradable and/or sorbed) and thereby constrain EDTA levels in a DBR.

SECTION 2. MgO SORPTION OF HUMIC ACIDS

Information Only

MgO will be positively charged at WIPP pH 9 and will sorb anions because its zero point of charge (ZPC) is pH ~ 12 (Kosmulski, 2016). Oxide surfaces are positively charged at pHs below their ZPC and negatively charged at pHs above their ZPC, which means oxide surfaces generally sorb anions from solution at pHs below their ZPC and cations at pHs above their ZPC (e.g. Stumm and Morgan, 1995). The ZPCs of a given metal oxide and hydroxide, e.g. MgO and $Mg(OH)_2$, are similar (e.g. Kosmulski, 2016) because oxide surfaces hydrate when exposed to solution. Consequently, the surface properties of a given metal oxide and hydroxide are typically very similar to one another. In the calculations below the surface chemistries of MgO and $Mg(OH)_2$ are therefore treated as being equal, as are the surface chemistries of Al_2O_3 and $Al(OH)_3$.

The total HA concentration used presently for WIPP, 2.0 mg/L, was originally measured for the CCA (DOE, 1996, Section 6.3.3.1) in experiments where 4 HAs were separately equilibrated with, or precipitated/coagulated from, brines containing Mg and Ca. "HA coagulation" and "HA solubility" are used interchangeably in the technical literature, though the two processes are different. Here the term "coagulation/solubility" is used to cover both. Wall and Matthews (2005) measured HA solubilities/coagulation from 95% GWB and 95% ERDA-6 brines but used a different HA than the ones used for the CCA measurements, and the brines had somewhat different compositions.

Wall and Matthews (2005) measured HA-MgO sorption from 95% GWB and 95% ERDA-6 brine initially containing 200 mg/L HA. In the absence of MgO, HA levels were ~ 17 mg/L (Wall and Matthews, 2005, Figures 4 and 5), roughly the solubility of HA measured separately (Wall and Matthews, 2005, Figure 2). The reduced HA solubility relative to distilled water is likely caused by the high Mg levels in the brines.

MgO dropped HA concentrations from ~ 17 to 0 – 2 mg/L (Figures 4 and 5 of Wall and Matthews, 2005). HA-MgO K_ds were calculated from the data as $K_{d,HA\text{-}MgO} = [HA_{initial}] - [HA_{final}]/[HA_{final}] \bullet C_{MgO}$; where C_{MgO} is the amount of MgO in the experiments (ml/g). HA-MgO K_ds are particularly sensitive to $[HA_{final}]$ because $[HA_{final}]$ was close to zero. Wall and Matthews' (2005) noted that HA was often sorbed to below the HA detection limit, but the HA detection limit wasn't clearly defined. If $[HA_{final}]$ was 2 mg/L, the calculated HA-MgO K_d range is 15 – 62 ml/g. If $[HA_{final}]$ was 1 mg/L, the HA-MgO K_d range would be 32 – 133 ml/g. Clearly to predict HA levels in the disposal area, a more certain value of the HA-MgO K_d than the K_d values of Wall and Matthews (2005) is needed, one measured to as low a HA detection limit as possible.

An HA-MgO K_d under WIPP conditions can be independently estimated starting from the work of Russell et al. (2009, Figure 3) who measured a HA-$Mg(OH)_2$ K_d of 160 ml/g in a pH 10.4, 0.016 M ionic strength solution. Normalizing Russell et al.'s (2009) K_d range from their higher surface

Information Only

area of $Mg(OH)_2$, 25 m^2/g, to the lower surface area of WIPP MgO (0.4 m^2/g), by multiplying by 0.4/25, indicates a HA-MgO K_d of 2.56 mL/g at pH 10.4, 0.016 M ionic strength.

Russell et al.'s (2009) K_ds must also be extrapolated to the lower pH and higher ionic strength of WIPP. This extrapolation is done by: 1. Deriving the HA-MgO K_d as a function of MgO surface charge, and; 2. Estimating MgO surface charge from Al_2O_3 surface charge. Step 2 is done to fill in MgO surface charge data gaps.

Step 1: HA sorbs as A- to positively charged MgO sites, $>MgOH_2^+$, by the following reaction,

$$A^- + >MgOH_2^+ \leftrightarrow >MgOH_2\text{-}A \qquad K_{eq} = [>MgOH_2\text{-}A]/[A^-][>MgOH_2^+],$$

where A^- is a carboxylate or phenolate group exposed on a HA surface, $>MgOH_2^+$ is a positively charged group on the MgO surface, $>MgOH_2$-A is an A^- sorbed to MgO, K_{eq} is the equilibrium constant for the sorption reaction, and brackets denote surface site concentrations (moles/M^2). By definition, the HA-MgO $K_d = [>MgOH_2\text{-}A]/[A^-]$, so $K_d = K_{eq}/[>MgOH_2^+]$. The last equation allows independently measured, or estimated, MgO surface charge, $[>MgOH_2^+]$, to be used to roughly estimate K_ds at other pHs and ionic strengths.

Step 2: $MgO/Mg(OH)_2$ has the same positive surface charge at one pH as Al_2O_3 has at a pH ~ 2 – 3.5 pH units lower (shown in Figure 1), this because the ZPC of Al_2O_3 is ~ 3 pH units lower than the ZPC of MgO, pH 9 vs. 12 (Kosmulski, 2016).

Combining Steps 1 and 2 leads to an expression whereby HA-MgO K_ds can be roughly extrapolated from MgO, or Al_2O_3, surface charge,

$$K_{d,X}/K_{d,Y} \sim [>MgOH_2^+]_Y/[>MgOH_2^+]_X \sim [>AlOH_2^+]_{Y,pH\text{-}3}/[>AlOH_2^+]_{X,pH\text{-}3},$$

where $K_{d,X}$ is an unknown HA-MgO K_d, $K_{d,Y}$ is a known HA-MgO K_d, $[>MgOH_2^+]_Y$ is the known amount of MgO positive surface charge for Y, $[>MgOH_2^+]_X$ is the known amount of MgO positive surface for X, $[>AlOH_2^+]_{Y,pH\text{-}3}$ is the known amount of Al_2O_3 surface charge for Y but 3 pH units lower, and $[>AlOH_2^+]_{X,pH\text{-}3}$ is the known amount of Al_2O_3 surface charge for X but 3 pH units lower.

Information Only

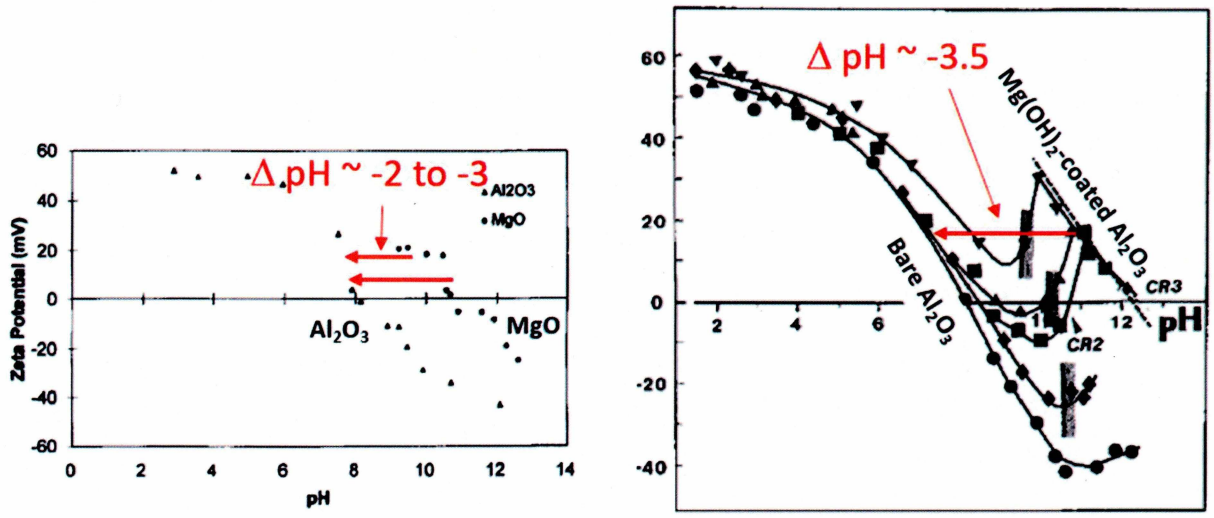


Figure 1. Al_2O_3 vs. MgO/$Mg(OH)_2$ surface charge (zeta potential). Left – Tari et al. (1997, Figure 2); Right – Pugh and Bergstrom (1988, Figure 2). Labelling added. Tari et al.'s (1997) measurements were done in 0.001 M KCl, Pugh and Bergstrom's were done in 0.01 M NaCl. Tari et al.'s (1997) MgO zeta potential measurements cease below pH 8.5 because of MgO dissolution.

This means that the increase in Al_2O_3 surface charge from pH 7.4 to pH 6 can be used to extrapolate Russell et al.'s (2009) pH 10.4 K_ds to WIPP pH 9. The measurements of Volkova et al. (2013, Figure 1) indicate that Al_2O_3 zeta potential (surface charge) increases ~ 80 % from pH 7.4 to pH 6 in 0.01 NaCl solutions, suggesting that Russell et al.'s (2009) pH 10.4 K_d would be 4.61 mL/g at pH 9, 0.016 M ionic strength.

Using the MgO – Al_2O_3 surface charge analogy to extrapolate the pH-adjusted K_d to WIPP brine ionic strength is done with the pH 6 AlOOH surface charge measurements of Tombacz et al. (2000, Figure 1) in 0.01, 0.1, and 1.0 M KNO_3 solutions. Linear extrapolation of these measurements predict an ~ 6.2-fold increase in the HA-MgO K_d going from 0.016 M to 6 M. The end result of the two pH-Al_2O_3-MgO-charge extrapolations for pH and ionic strength is a pH 9, 6 M ionic strength estimated HA-MgO K_d of 28.8 mL/g, in the range of K_ds calculated from Wall and Matthews' (2005) data assuming a HA detection limit of 2 mg/L.

Other WIPP Humic Model Conservatisms

The conservatisms in the WIPP HA model have been documented by Mariner (2016, 2018, 2019, 2023) and Mariner and Sassani (2014). In addition to assuming all humic colloids are HA (no fulvic acid); HA-An complexation is over-estimated; and HA-Mg and HA-Ca complexation is under-estimated. HA has a significantly greater affinity for Ans than fulvic acid, but humic colloids in natural groundwaters are a combination of both (Mariner and Sassani, 2014). The

Information Only

stability constants used for HA-An complexation in the WIPP HA model were derived at one molar ionic strength and were not adjusted to the higher ionic strength of WIPP brines; high ionic strength tends to reduce HA-An complexation (Mariner, 2016). To ensure that HA-bound An concentrations are not underestimated in PA calculations, the stability constants for HA-Ca and HA-Mg complexes were set significantly lower than observed at the expected high ionic strength and pH of MgO-equilibrated WIPP brines (Mariner, 2016).

Uncertainty/Conservatism Reduction

The Wall and Matthews (2005) experiments might be redone at lower HA concentrations (Mariner and Sassani, 2014), and a lower HA detection limit, to measure a more accurate K_d. Using ^{131}I-labelled HA, for example, would allow much better resolution of HA levels than measuring TOC levels (e.g. Marquardt, 2004, pg. 193), resulting in more accurate HA-MgO K_ds.

SECTION 3. MgO SORPTION OF MICROBES

MgO should sorb microbes at WIPP as the same reaction is used to remove microbes (microalgae) from wastewater (Folkman and Wachs, 1973, Smith and Davis, 2012); positively charged $Mg(OH)_2$ surfaces sorb microalgae through microalgae surface carboxylate and phenolate groups, and subsequently flocculate them. Sorption of microbial colloids to fixed substrates is not presently included by PA (DOE, 2019, SOTERM-22).

No microbe-MgO sorption measurements exist for high ionic strength, pH 9 WIPP brine. But they can be estimated from the *Bacillus subtilis*-Al_2O_3 K_ds calculated from the measurements of Yee et al. (2000) once they are adjusted for the higher positive surface charge of MgO by the Al_2O_3-MgO surface charge analogy used above for HA-MgO sorption, and for the higher ionic strength of WIPP (~ 6 M) compared to the 0.01 M ionic strength of Yee et al.s (2000) experiments on *Bacillus subtilis*. Because the surface charge of different species of bacteria is similar (Hadjoudja, 2010, Table 3), K_ds measured or estimated for *Bacillus subtilis* are assumed to apply to halophilic WIPP microbes as well.

Figure 2 shows *Bacillus subtilis* – Al_2O_3 sorption measurements of Yee et al. (2000). Yee et al. (2000) measured ~ 30 % *Bacillus subtilis* sorption at pH 6, 0.01 M $NaNO_3$ (10 g/L of Al_2O_3, 2 g/L *Bacillus subtilis*); a repeat experiment showed ~ 62 % sorption at pH 5.9, 0.01 M $NaNO_3$ (Yee, 2000, Figure 7). The two measurements are equivalent to a pH 9 microbe-MgO K_d range of 43 – 163 mL/g. But these values must be adjusted downwards to the high salinity of WIPP brine since Yee et al. (2000) measured an ~ 30% decrease in microbe sorption over a 3 order of magnitude increase in ionic strength. Extrapolating Yee et al.'s (2000) experiments from their ionic strength of 0.01 M to WIPPs ionic strength of 6 M (Figure 2), predicts that the % microbes sorbed by MgO at pH 9 must be reduced by ~ 50 %, from 30 – 62 % microbe sorbed from 0.01 M $NaNO_3$ to 15 – 31 % microbe sorbed from WIPP brine. This is equivalent to a microbe-MgO K_d

Information Only

range of 18 - 45 mL/g. This would lower microbe levels by a factor of 21 – 52 in the disposal area, assuming the latter is well-mixed.

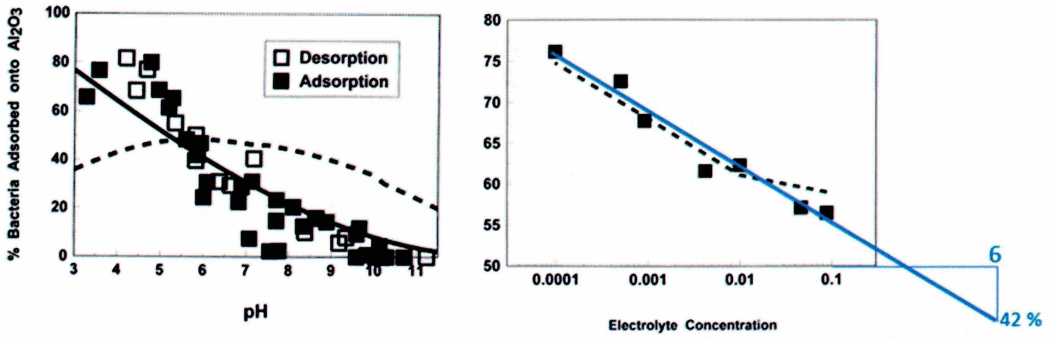


Figure 2. *Bacillus subtillus* adsorption measurements of Yee et al. (2000). Left – Figure 2 of Yee et al. (2000), 0.01 M $NaNO_3$, 10 g/l of mineral, 2 g/l of bacteria; right – Figure 7 of Yee et al. (2000), pH 5.9, 10 g/l of mineral, 2 g/l of bacteria. Ionic strength extrapolation (blue line) added.

There is more than sufficient MgO surface area to sorb WIPP microbes. Using the MgO/brine ratio at WIPP, 1164 g/L (calculated after the analysis of Domski, 2023), assuming a WIPP MgO surface area of 0.4 m^2/g, and a WIPP microbe, e.g. *Halobacterium sp.*, dimension of 5 μm x 1 μm x 1 μm, suggests a microbe sorption capacity of 9e10 cells/ml; almost two orders of magnitude higher than the highest microbe population expected at WIPP, 10^9 cells/ml (Reed et al., 2013).

Lastly, MgO sorption of HAs, microbes, and phosphate should not impair MgO lowering of CO_2 levels because their summed net is calculated to occupy a minor fraction of the initially available MgO surface sites. The initially available MgO surface site concentration is calculated to be 1.8e-3 M (again assuming a surface site density of 2.3 sites/nm^2). Sorption of 2 mg/L HA, the amount of HA expected in the CCA in the absence of sorption, is estimated to occupy 9e-6 M of MgO sites, though it is not clear if MgO sorption of HA would prompt dissolution/resuspension of HA elsewhere in the disposal area leading to higher loading. Sorption of 10^9 cells/ml, the high-end microbial population expected by Reed et al. (2013), is calculated to occupy 1.9e-5 M of MgO sites. Dissolved phosphate levels, if set by hydroxylapatite solubility, would be 1.2e-7 M (Appendix). This assumes that hydroxylapatite growth will occur from Ca-containing WIPP brines in contact with waste inside crushed packages before phosphate can contact MgO outside the packages.

Uncertainty Reduction

Actual measurements of microbe-MgO K_ds are needed. Microbe-MgO sorption might be measured in WIPP brine to as low a microbe detection limit as possible.

Information Only

SUMMARY

The Chemistry Conceptual Model of the CCA is indeed conservative in predicting mobile An and microbe levels in the disposal area. The last two columns of Table 4 suggest that the present solubility-based WIPP model conservatively overpredicts dissolved Th by a factor of 5, Pu(III) by a factor of 200, Pu(IV) by a factor of ~ 3, and Am by more than 4 orders of magnitude.

If the WIPP Pu inventory were assumed to be 100 % Pu(III), the sorption-predicted dissolved Pu levels would be 3.6e-8, almost a hundred times less than the 50:50 Pu(IV):Pu(III) predicted Pu solubility of 3.4e-6 because An(III)s sorb more strongly to corrosion products than An(IV)s.

Also, the microbe levels available for mobilizing Ans in the current WIPP model are conservative because they may be at least an order of magnitude too high.

To improve the sorption analysis, the following might be done, listed in order of importance:

1. Measure An(III) and An(IV) K_ds for hibbingite (and/or magnetite and green rust) under WIPP conditions at low and high An surface loadings, and corrosion product surface areas measured from WIPP steel corrosion experiments,

2. Measure An(III) and An(IV) K_ds for anaerobically degraded dunnage under WIPP conditions at high An surface loadings,

3. Develop sorption analyses for the waste solids not considered here - Other Inorganic Material, Solidified Inorganic Material, Plastic, Lead, Cellulose, Solidified Organic Material, and Other Metal/Alloys,

4. Measure An-hydrocerussite K_ds in WIPP brine,

5. Constrain WIPP EDTA levels by examining the setting and history of the individual WIPP EDTA waste streams, and

6. Measure HA and microbe sorption to MgO in WIPP brine to low detection limits.

The importance of measuring sorbate concentrations to the lowest detection limit possible cannot be over-emphasized. Many of the K_ds used above are <u>minimum</u> K_ds because they were measured at or below the sorbate detection limit. The K_ds could be higher, and the calculated reduction of mobile Ans greater. The exception is the K_d measurements that might be done for the Surplus Pu package analysis (Number 2 above); these need to be done at high surface loadings.

Information Only

Lastly, the calculation of ample sorption capacity in Surplus Pu CH-waste suggests that waste heterogeneity would not change the overall conclusion that sorption will keep An concentrations below solubility limits, often by orders of magnitude.

Information Only

APPENDIX: PHOSPHATE IN THE DISPOSAL AREA

As shown above, the absence of sorption in the current WIPP model substantially over-predicts dissolved levels of the individual Ans, likely dwarfing the potential impacts of phosphate reaction in the disposal area discussed below. If sorption is not included in a future WIPP model, all the conclusions of this Appendix apply.

The current Chemistry Conceptual Model does not include reaction of waste phosphate with Ans, or passivation of Fe and Pb metal by phosphate. Yet when added to contaminated soils or at hazardous waste sites, phosphate sharply limits dissolved concentrations of metals and Ans (e.g. Jensen et al., 1996, Zhou et al., 2015, Selim and Magdi, 2018) by forming low solubility metal/An phosphates and/or by forming metal/An-sorbing hydroxylapatite. Phosphate released from the waste at WIPP might similarly reduce dissolved An levels in the WIPP disposal area.

387 metric tons of phosphate will be disposed of in WIPP (Van Soest, 2022), primarily as residue from the bismuth-phosphate, REDOX, and PUREX processes used to separate uranium and plutonium, and miscellaneous detergents such as tri-polyphosphate. The detergent phosphate should become available quickly in the disposal area as there are no C-O-P bonds to cleave.

The REDOX and PUREX processes used tributyl phosphate (TBP); REDOX and PUREX process waste is an important fraction of the waste coming to WIPP. TBP breakdown occurs through sequential loss of butyl groups from TBP to dibutyl phosphate (DBP), to monobutyl phosphate (MBP), to phosphate. The DBP to MBP step is the slowest step (Burger, 1955). Breakdown of TBP at pH 9 was measured at 80°C to have a pseudo-first order rate constant of 4e-3 hr^{-1} (Liu et al., 2018). Using an activation energy of 14 kcal/mol for hydrolysis in near neutral solutions (Burger, 1955) points to a pH 9 25°C TBP breakdown rate of 1e-4 hr^{-1}, rates being proportional to the solubility-limited dissolved concentration of TBP, 0.4 g/L, meaning an overall TBP breakdown rate of 4e-5 g/L·hr. Other factors that could increase the rate of phosphate release from TBP include microbial biodegradation (e.g. Thomas and Macaskie, 1998, Berne et al., 2004, Liu et al., 2019) and alpha radiolysis (e.g. Barney and Bouse, 1977, Mincher et al., 2009), conversion of TBP to DBP increasing with radiolytic dose, depending on the TBP diluent.

Some caveats are in order. The 4e-5 g/L·hr rate calculated above describes breakdown of TBP to DBP, which breaks down to phosphate more slowly. For example, an acidic uranium nitrate-containing solution the DBP conversion rate to MBP was $^1/_3$ to $^1/_2$ the rate of TBP conversion to DBP (Burger, 1955). The effects of other waste components (or binders), or TBP aging, might also affect rates, as might the components of the WIPP brine.

Using this approximate rate, an estimate for complete conversion of REDOX + PUREX TBP to phosphate in the WIPP disposal area is 32 years. The calculation assumes that half of the WIPP phosphate inventory is TBP by mass, the rest being presumably phosphate-insoluble bismuth-

Information Only

phosphate waste, and that the DBP to phosphate conversion rate is $^1/_2$ the TBP to DBP conversion rate. Dissolving the available phosphate into the minimum DBR volume gives an available phosphate level of 7e-4 M after 32 years. But hydroxylapatite and $AmPO_4$(am) would grow at much lower phosphate levels. Hydroxylapatite is a strong sorber of Ans from WIPP brines; Krumhansl (1996) measured sorption K_ds onto hydroxylapatite of $10^{2.3\text{-}6.1}$ mL/g for Am and $10^{0.9\text{-}4.3}$ mL/g for Pu.

The important points here are that relatively low levels of phosphate are needed to lower Am solubility and produce Am and Pu-sorbing hydroxylapatite, and that these levels might be reached soon after closure.

Corrosion Inhibition

Phosphate inhibition of Fe and Pb corrosion will probably not occur in the WIPP disposal area because hydroxylapatite growth will limit phosphate to lower levels than required for corrosion inhibition. Pb corrosion under oxidizing conditions in pipes is inhibited by ~3 mg/L phosphate; Fe pipe corrosion under oxidizing conditions is inhibited by 0.5 to 3 mg/L phosphate (AWWARF, 1996), 1.6 – 9.7e-5 M. Phosphate levels will be lower than these values in Ca-rich WIPP brine because of hydroxylapatite growth. Also, phosphate passivation of Fe surfaces would be less effective under the reducing conditions of WIPP. Phosphate passivation of steel surfaces under oxidizing conditions is caused by the formation of a semi-impervious coating of ferric phosphate. Under the reducing conditions of WIPP, a less impervious corrosion layer of vivianite, ferrous phosphate, will form. Moreover, under reducing conditions phosphate actually accelerates corrosion of steel by microbial attack (Munoz et al., 2007).

Uncertainty Reduction

Depending on inclusion of sorption in a future WIPP model, work that might be done to quantify the disposal area impacts of phosphate are to:

1. Develop a more precise inventory of WIPP phosphate sources including $BiPO_4$, TBP, and fast-reacting polyphosphates,

2. Measure TBP breakdown rates under WIPP conditions including the presence of waste and binders and biodegradation.

Information Only

REFERENCES

AWWARF (1996) Internal corrosion of water distribution systems. AWWARF-DVGW-TZW cooperative research report, Denver, CO, 586 pp.

Baes Ill, C. F., and R. D. Sharp. "A proposal for estimation of soil leaching and leaching constants for use in assessment models." Journal of Environmental Quality 12, no. 1 (1983): 17-28.

Barney, G. Scott, and D. G. Bouse. *Alpha radiolysis of tributyl phosphate: effect of diluents*. No. ARH-ST--153. Atlantic Richfield Hanford Co., 1977.

Berl, E., and W. Koerber. "Fermentation of cellulose and cellulose humic acid and lignin and lignin humic acid." Journal of the American Chemical Society 60, no. 7 (1938): 1596-1598.

Berne, Cécile, Blandine Montjarret, Yasmina Guountti, and Daniel Garcia. "Tributyl phosphate degradation by Serratia odorifera." Biotechnology letters 26 (2004): 681-686.

Blesa, Miguel A., Elena B. Borghi, Alberto JG Maroto, and Alberto E. Regazzoni. "Adsorption of EDTA and iron—EDTA complexes on magnetite and the mechanism of dissolution of magnetite by EDTA." Journal of Colloid and Interface Science 98, no. 2 (1984): 295-305.

Burger, L. L. "The Chemistry of Tributyl Phosphate: A Review." (1955). From OSTI.GOV.

Byegård, J., G. Skarnemark, and M. Skålberg. "The stability of some metal EDTA, DTPA and DOTA complexes: Application as tracers in groundwater studies." Journal of radioanalytical and nuclear chemistry 241, no. 2 (1999): 281-290.

Cantrell, K. J., and R. G. Riley "Subsurface Behavior of Plutonium and Americium at Non-Hanford Sites and Relevance to Hanford". PNNL-17386. 2008.

Carlsen, Lars, and O. Platz. "Retention of radionuclides in halite and anhydrite." *European Applied Research Reports: Nuclear Science and Technology Section* 7, no. 4 (1986): 539-575.

Davis, James A., and Douglas B. Kent. "Surface complexation modeling in aqueous geochemistry." Reviews in mineralogy and geochemistry 23, no. 1 (1990): 177-260.

DOE. 1996. Title 40 CFR Part 191 Compliance Certification Application for the Waste Isolation Pilot Plant, Appendix SOTERM.

DOE, 2013. DOE/CBFO 11-3478 Rev 0, Planned Change Request, Waste Isolation Pilot Plant Repository Reconfiguration.

DOE 2019. Appendix SOTERM.

Domski, P. S. 2023. Prediction of Baseline Actinide Solubilities for the Replacement Panels Planned Change Request (RPPCR) Performance Assessment. ERMS579503.

Dosch, R. G., and A. W. Lynch. *Interaction of radionuclides with geomedia associated with the Waste Isolation Pilot Plant (WIPP) site in New Mexico*. No. SAND-78-0297. Sandia National Lab.(SNL-NM), Albuquerque, NM (United States), 1978.

Information Only

Farr, J. Douglas, Roland K. Schulze, and Bruce D. Honeyman. "Aqueous Pu (IV) sorption on brucite." *Radiochimica Acta* 88, no. 9-11 (2000): 675-680.

Farr, John Douglas, Mary P. Neu, Roland K. Schulze, and Bruce D. Honeyman. "Plutonium uptake by brucite and hydroxylated periclase." *Journal of alloys and compounds* 444 (2007): 533-539.

Folkman, Y. A. M. Wachs. 1973. "Removal of algae from stabilization pond effluents by lime treatment." Water Research pp. 419-435.

Grambow, Bernd, M. López-García, J. Olmeda, M. Grivé, Nicolas CM Marty, S. Grangeon, F. Claret et al. "Retention and diffusion of radioactive and toxic species on cementitious systems: Main outcome of the CEBAMA project." Applied geochemistry 112 (2020): 104480.

Guo, Xiaofang, Zebin Wei, and Qitang Wu. "Degradation and residue of EDTA used for soil repair in heavy metal-contaminated soil." Transactions of the Chinese Society of Agricultural Engineering 31, no. 7 (2015): 272-278.

Hadjoudja, S., Véronique Deluchat, and Michel Baudu. "Cell surface characterisation of Microcystis aeruginosa and Chlorella vulgaris." Journal of colloid and interface science 342, no. 2 (2010): 293-299.

Hakem, N. L., P. G. Allen, and E. Sylwester "Effect of EDTA on plutonium migration." Journal of Radioanalytical and nuclear Chemistry 250, no. 1 (2001): 47-53.

Jensen, Mark P., Kenneth L. Nash, Lester R. Morss, Evan H. Appelman, and Mark A. Schmidt. "Immobilization of actinides in geomedia by phosphate precipitation." Chapter 17 pp 272-285, in Humic and Fulvic Acids - Isolation, Structure, and Environmental Role. Editor(s): Jeffrey S. Gaffney, Nancy A. Marley, and Sue B. Clark. ACS Symposium Series.

King, S. 2021, 12/20/21 Memo: Repository volume, DRZ volume, and minimum brine volume for a direct brine release for a repository with new panels. ERMS576475.

King, S. 2023, 8/14/23 Memo: Actinide Solubility and Colloidal Contributions in the CRA-2024. ERMS580242.

Kosmulski, Marek. "Isoelectric points and points of zero charge of metal (hydr) oxides: 50 years after Parks' review." Advances in Colloid and Interface Science 238 (2016): 1-61.

Krumhansl, J. L., K. M. Kimball, and C. L. Stein. "A review of WIPP (Waste Isolation Pilot Plant) repository clays and their relationship to clays of adjacent strata." (1990). From OSTI.GOV.

Krumhansl, J. L. (1996) Summary of Apatite K_d Work. May 29, 1996. Sandia National Laboratories Memo.

Lin, Peng, Min Chen, and Laodong Guo. "Effect of natural organic matter on the adsorption and fractionation of thorium and protactinium on nanoparticles in seawater." *Marine Chemistry* 173 (2015): 291-301.

Information Only

Liu, Jia, Langping Wu, Steffen Kümmel, Jun Yao, Thomas Schaefer, Hartmut Herrmann, and Hans-Hermann Richnow. "Carbon and hydrogen stable isotope analysis for characterizing the chemical degradation of tributyl phosphate." Chemosphere 212 (2018): 133-142.

Liu, Jia, Hai Lin, Yingbo Dong, and Bing Li. "Elucidating the biodegradation mechanism of tributyl phosphate (TBP) by Sphingomonas sp. isolated from TBP-contaminated mine tailings." *Environmental Pollution* 250 (2019): 284-291.

Luckscheiter, B., and B. Kienzler. "Determination of sorption isotherms for Eu, Th, U and Am on the gel layer of corroded HLW glass." *Journal of nuclear materials* 298, no. 1-2 (2001): 155-162.

Maragkou, Eleni, and Ioannis Pashalidis. "Investigations on the interaction of EDTA with calcium silicate hydrate and its impact on the U (VI) sorption." Coatings 11, no. 9 (2021): 1037.

Mariner, P. E. (2016). Actinide(IV)-Humic Complexation in the WIPP Performance Assessment. Sandia National Laboratories, Carlsbad, New Mexico. ERMS567222.

Mariner, P. E. (2018). Actinide(III)-Humic Complexation in the WIPP Performance Assessment. Sandia National Laboratories, Carlsbad, New Mexico. ERMS569599.

Mariner, P. E. (2019). A summary of humic colloid parameter values to be implemented in the CRA-2019 Deferred Performance Assessment. Sandia National Laboratories, Carlsbad, New Mexico. ERMS571250.

Mariner. P.E., (2023). Updates to the WIPP humic Colloids models for An(III) and An(IV). July 26, 2023. Albuquerque, NM: Sandia National Laboratories. ERMS 580251.

Mariner, Paul E., and David Carl Sassani. Analysis report for WIPP colloid model constraints and performance assessment parameters. No. SAND2014-1961. Sandia National Lab. (SNL-NM), Albuquerque, NM (United States), 2014.

Marquardt, C. M. (Editor) "Investigations on the Complexation Behaviour of Humic Acids and Their Influence on the Migration of Radioactiv and Non-radioactive Substances Under Conditions Close to Nature". Forschungszentrum Karlsruhe in der Helmholtz-Gemeinschaft Wissenschaftliche Berichte, FZKA 6999 (2004) (https://publikationen.bibliothek.kit.edu/270059161/3814573).

Means, Jeffrey L., Tanya Kucak, and David A. Crerar. "Relative degradation rates of NTA, EDTA and DTPA and environmental implications." Environmental Pollution Series B, Chemical and Physical 1, no. 1 (1980): 45-60.

Mincher, Bruce J., Giuseppe Modolo, and Stephen P. Mezyk. "The effects of radiation chemistry on solvent extraction: 1. Conditions in acidic solution and a review of TBP radiolysis." Solvent Extraction and Ion Exchange 27, no. 1 (2009): 1-25.

MSHA - Mine Safety and Health Administration, Dec 1, 2016 Memo from Christopher Mark. Field Investigation at the U.S. Department of Energy's Waste Isolation Pilot Plant (WIPP), ID No. 29-01857, Carlsbad, New Mexico (RCD Control Number 17AAO1).

Information Only

Morelová, Nikoleta. "Steel corrosion and actinide sorption by iron corrosion products under saline conditions." PhD diss., Karlsruher Institut für Technologie (KIT), 2020.

Munoz, Leonardo De Silva, Alain Bergel, and Régine Basséguy. "Role of the reversible electrochemical deprotonation of phosphate species in anaerobic biocorrosion of steels." Corrosion science 49, no. 10 (2007): 3988-4004.

Nalet, Camille, and André Nonat. "Ionic complexation and adsorption of small organic molecules on calcium silicate hydrate: Relation with their retarding effect on the hydration of C3S." Cement and Concrete Research 89 (2016): 97-108.

National Academies of Sciences, Engineering, and Medicine. "Review of the Department of Energy's Plans for Disposal of Surplus Plutonium in the Waste Isolation Pilot Plant." (2020).

Nemer, Martin B., Yongliang Xiong, Ahmed E. Ismail, and Je-Hun Jang. "Solubility of $Fe_2(OH)_3Cl$ (pure-iron end-member of hibbingite) in NaCl and Na_2SO_4 brines." Chemical Geology 280, no. 1-2 (2011): 26-32.

Ochs, Michael, Dirk Mallants, and Lian Wang. *Radionuclide and metal sorption on cement and concrete*. Vol. 2. Berlin/Heidelberg, Germany: Springer, 2016.

Park, Sang-Won, James O. Leckie, and Malcolm D. Siegel. Surface complexation modeling of uranyl adsorption on corrensite from the Waste Isolation Pilot Plant site. No. SAND--90-7084. Sandia National Labs., 1995.

Pugh, R. J., and L. Bergström. "The uptake of Mg (II) on ultrafine α-silicon carbide and α-alumina." Journal of colloid and interface science 124, no. 2 (1988): 570-580.

Reed, Donald T. Actinide Solubility and Speciation in the WIPP [PowerPoint]. No. LA-UR-15-28106. Los Alamos National Lab.(LANL), Los Alamos, NM (United States), 2015.

Reed, D. T, J. Swanson, J. Lucchini, M. Richmann. Intrinsic, Mineral and Microbial Colloid Enhancement Parameters for the WIPP Actinide Source Term. LANL-CO ACRSP, LCO-ACP-18, LA-U R 13-20858, 2013.

Reedlunn, Benjamin, and James Bean. Simulations of Pipe Overpack Container Compaction at the Waste Isolation Pilot Plant. No. SAND2019-12111. Sandia National Lab.(SNL-NM), Albuquerque, NM (United States), 2019.

Russell, Caroline G., Desmond F. Lawler, Gerald E. Speitel Jr, and Lynn E. Katz. "Effect of softening precipitate composition and surface characteristics on natural organic matter adsorption." Environmental science & technology 43, no. 20 (2009): 7837-7842.

Selim, H. Magdi, ed. Phosphate in soils: interaction with micronutrients, radionuclides and heavy metals. CRC Press, 2018.

Seliman, A. F., E. H. Borai, Y. F. Lasheen, M. M. Abo-Aly, T. A. DeVol, and B. A. Powell. "Mobility of radionuclides in soil/groundwater system: Comparing the influence of EDTA and four of its degradation products." Environmental Pollution 158, no. 10 (2010): 3077-3084.

Information Only

Serne, R. J., A. R. Felmy, K. J. Cantrell, K. M. Krupka, J. A. Campbell, H. Bolton Jr, and J. K. Fredrickson. "Characterization of radionuclide-chelating agent complexes found in low-level radioactive decontamination waste. Literature review." NUREG/CR-6124, PNNL-8856 (1996).

Smith, Benjamin T., and Robert H. Davis. "Sedimentation of algae flocculated using naturally-available, magnesium-based flocculants." Algal Research 1, no. 1 (2012): 32-39.

Stumm, W. and J. J. Morgan. Aquatic chemistry: chemical equilibria and rates in natural waters. Wiley-Interscience (1995).

Swanson, Juliet Stumpf, Diana M. Norden, Hnin M. Khaing, and Donald T. Reed. "Degradation of organic complexing agents by halophilic microorganisms in brines." Geomicrobiology Journal 30, no. 3 (2013): 189-198.

Tari, G., J. M. F. Ferreira, and O. Lyckfeldt. "Influence of magnesia on colloidal processing of alumina." Journal of the European Ceramic Society 17, no. 11 (1997): 1341-1350.

Thibault, D. H., M. I. Sheppard, and P. A. Smith. *A critical compilation and review of default soil solid/liquid partition coefficients, Kd, for use in environmental assessments*. No. AECL--10125. Atomic Energy of Canada Ltd., 1990.

Thomas, Russell AP, Andy P. Morby, and Lynne E. Macaskie. "The biodegradation of tributyl phosphate by naturally occurring microbial isolates." *FEMS microbiology letters* 155, no. 2 (1997): 155-159.

Thomas, Russell AP, and L. E. Macaskie. "The effect of growth conditions on the biodegradation of tributyl phosphate and potential for the remediation of acid mine drainage waters by a naturally-occurring mixed microbial culture." Applied microbiology and biotechnology 49 (1998): 202-209.

Thomas, Jeffrey J., Hamlin M. Jennings, and Andrew J. Allen. "The surface area of hardened cement paste as measured by various techniques." Concrete Science and Engineering 1, no. 1 (1999): 45-64.

Tiruta-Barna, Ligia, and Nicoleta Schiopu. "Modelling inorganic biocide emission from treated wood in water." *Journal of hazardous materials* 192, no. 3 (2011): 1476-1483.

Tombacz, E., A. Dobos, M. Szekeres, H. D. Narres, E. Klumpp, and I. Dekany. "Effect of pH and ionic strength on the interaction of humic acid with aluminium oxide." Colloid and Polymer Science 278 (2000): 337-345.

Van Soest, G. D. 2022. Performance Assessment Inventory Report – 2022. INV-PA-2022, Revision 0. Carlsbad, NM: Los Alamos National Laboratory.

Volkova, A. V., L. E. Ermakova, E. V. Golikova, and N. F. Bogdanova. "Electrokinetic properties of aluminum oxide nanodispersions in NaCl solutions." *Colloid Journal* 75 (2013): 49-58.

Wall, Nathalie A., and Sara A. Mathews. "Sustainability of humic acids in the presence of magnesium oxide." *Applied Geochemistry* 20, no. 9 (2005): 1704-1713.

Information Only

Wang, Z., R. C. Moore, A. R. Felmy, M. J. Mason, and R. K. Kukkadapu. "A study of the corrosion products of mild steel in high ionic strength brines." Waste management 21, no. 4 (2001): 335-341.

Wen, Jia, Samuel P. Stacey, Mike J. McLaughlin, and Jason K. Kirby. "Biodegradation of rhamnolipid, EDTA and citric acid in cadmium and zinc contaminated soils." Soil Biology and Biochemistry 41, no. 10 (2009): 2214-2221.

Yee, Nathan, Jeremy B. Fein, and Christopher J. Daughney. "Experimental study of the pH, ionic strength, and reversibility behavior of bacteria–mineral adsorption." Geochimica et Cosmochimica Acta 64, no. 4 (2000): 609-617.

Zhou, Shiwei, Zhengguo Song, Minggang Xu, and Shibao Chen. "Effect of phosphate addition on mobility and phytoavailability of heavy metals in soils." In Phosphate in Soils: Interaction with Micronutrients, Radionuclides and Heavy Metals, pp. 203-235. CRC Press, 2015.

Information Only

1. The calculations herein are used for the document: WHITE PAPER: SORPTION AND THE WIPP CHEMISTRY CONCEPTUAL MODEL by Pat Brady
2. Color-coding: Yellow = outputs, Blue = user-adjusted variable; Green = important internally calculated inputs, No shading = inputs.
3. 'see text' refers to the document in item 1.

Information Only

TOTAL REP CALC'S

Input Kd's and g/ml of waste components

		all kd's in ml/g		base kd's	[w.edta]kd's
		soil-g	7.98E+09		
		cement-g	1.52E+09		
		kd-am-soil	810	810	71
Assumed		kd-pu-soil	60000	60000	
Corrosion, Fines		kd-am-cem	1.00E+04	1.00E+04	877
Xcorrosion	0	kd-pu-cem	3.00E+04	3.00E+04	
Xfine-salado	0.01	kd-am-hibb	1.00E+06	1.00E+06	87700
		kd-pu-hibb	1.00E+05	1.00E+05	
		real-salado-kd	949	949	86
		real-salado-kd	825	825	

	rep
hib-g/ml	3.918
soil-g/ml	0.236
cem-g/ml	0.045
salado-g/ml	204.734 DRZ

NOTES:
1. For all but inventory calcs, Pu means An4, Am means An3, except where explicitly stated - e.g. in the Pu3/Pu4 calcs.
2. 'mox' means surplus Pu. 'rep' means repository [no DRZ].

Calculation of real Salado fines Kd [1% clay, 10% CaSO4, rest NaCl]

Kd-Am-1%	920	1800	39 Avg. of Dosch and Lynch [1978] table 8 and 12 values, Brine B.
Kd-Pu-1% c	155	100	211
kd-am-10%	29	Brine B values from Dosch and Lynch [1978], Table 11.	
kd-pu-10%	670		
real-salado	949		
real-salado	825		

Calculation of g/ml of hibbingite in rep.

MW Hibb	198.153
7.47E+10	g_fe
1.34E+09	mol-fe
6.69E+08	mol-hib
1.32E+11	g-hib
3.918E+00	g/ml-hib

Mass-weighted sorption calculation, total rep [1st equation in txt]

Inventory [Reed, 2015 and NAS, 2020]

	kg	moles	
th	1.35E+04	5.87E+04	
pu	5.10E+04	2.13E+05	w. mox
am	203	835	
	TOTAL	2.72E+05	
sites neede	M2	7.16E+10	

	mol/L no sorptior	[co-c]/c	mol/L after-sorp	mol/L edta	24285.71
th	1.74E-03	17195	1.0E-07	1.3E-07	
pu3	3.14E-03	2581	1.2E-06	1.2E-06	
pu4	3.14E-03	17195	1.8E-07	2.4E-07	
am	2.47E-05	2580	9.6E-09	9.6E-09	

CH-MOX BBL CALC'S

Contents 55 gal mox drum

18120	g-fe		
324.44	mol fe		
3.21E+04	g-hibbingite		
1.05E+05	g-org		
4.21E+05	m2 hibb/cco	Xcorr	0.5
1.62E+00	sites hibb/pkg		
29878.02552	ml-squashed drum		
1.65E+00	sites-hibb-mol	cons-void-vol	
1.16E+01	sites-org-mol	0.14352	

Input Kd's and g/ml of waste components

kd's		
1.00E+06	cp-kd-am	pu3
1.00E+05	cp-kd-th	Lin et al. 2015, Table 1, ; pu4
1.12E+05	org-kd-am	Thibault et al. 1990
1.75E+05	org-kd-th	Lin et al. Table 1, ha, no nnp
2.06E+00	hibb - g/ml	
6.72E+00	org-g/ml	

Mass-weighted sorption calculation, CH-MOX bbl [2nd equation in text]

co [mol/l]	[co-c]/c
2.1E-02	1.2E-08
2.1E-02	1.6E-08

Convert eq-HA-wood to eq-HA

5.00E-03	eq-HA/g-HA	crboxylate+phenolate avg Marquardt et al., Table 1
1.10E-04	eq-HA/g-wooc	Tiruta-Barna, 2011
4.55E+01		

REFERENCES

Dosch, R. G., and A. W. Lynch. *Interaction of radionuclides with geomedia associated with the Waste Isolation Pilot Plant (WIPP) site in New Mexico*. No. SAND-78-0297. Sandia National Lab.(SNL-NM), Albuquerque, NM (United States), 1978.

Lin, Peng, Min Chen, and Laodong Guo. "Effect of natural organic matter on the adsorption and fractionation of thorium and protactinium on nanoparticles in seawater." *Marine Chemistry* 173 (2015): 291-301.

Marquardt, C. M. (Editor) "Investigations on the Complexation Behaviour of Humic Acids and Their Influence on the Migration of Radioactiv and Non-radioactive Substances Under Conditions Close to Nature". Forschungszentrum Karlsruhe in der Helmholtz-Gemeinschaft Wissenschaftliche Berichte, FZKA 6999 (2004) (https://publikationen.bibliothek.kit.edu/270059161/3814573).

National Academies of Sciences, Engineering, and Medicine. "Review of the Department of Energy's Plans for Disposal of Surplus Plutonium in the Waste Isolation Pilot Plant." (2020).

Reed, Donald T. Actinide Solubility and Speciation in the WIPP [PowerPoint]. No. LA-UR-15-28106. Los Alamos National Lab.(LANL), Los Alamos, NM (United States), 2015.

Thibault, D. H., M. I. Sheppard, and P. A. Smith. *A critical compilation and review of default soil solid/liquid partition*

Information Only

Calculation of HA-MgO Kd's from Wall and Matthews (2005) data, Figures 2 and 5

g-liq/g-mg	g-mgo/ml-l	co	c	Kd
2.4	0.5	17	2	15.0
10	0.12	17	2	62.5
2.4	0.5	17	1	32.0
10	0.12	17	1	133.3
2.4	0.5	17	0.1	338.0
10	0.12	17	0.1	1408.3

WM, 2005
2.4 and 10 g-liqu/g-mgo
assume liqu density = 1.2 g/cc

Extrapolation of Russell et al.'s (2009) HA-MgO Kd to WIPP MgO-Brine

0.16	L/g	LAHS Kd
160	ml/g	LAHS Kd
2.6	SA-normalized	see text
4.6	pH-normalized	see text
28.8	tds-normalized	see text, and to right

8.333333
0.12

REFERENCES

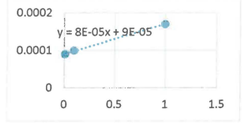
Wall, Nathalie A., and Sara A. Mathews. "Sustainability of humic acids in the presence of magnesium oxide." *Applied Geochemistry* 20, no. 9 (2005): 1704-1713.

Russell, Caroline G., Desmond F. Lawler, Gerald E. Speitel Jr, and Lynn E. Katz. "Effect of softening precipitate composition and surface characteristics on natural organic matter adsorption." Environmental science & technology 43, no. 20 (2009): 7837-7842.

Tombacz, E., A. Dobos, M. Szekeres, H. D. Narres, E. Klumpp, and I. Dekany. "Effect of pH and ionic strength on the interaction of humic acid with aluminium oxide." Colloid and Polymer Science 278 (2000): 337-345.

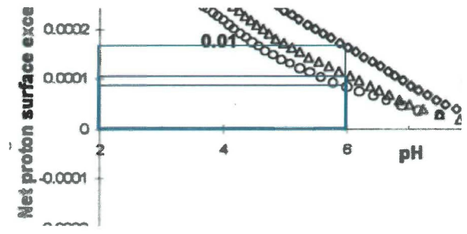
Fit of Tombacz et al. (2000) pH 6 boehmite surface charge data, figure 1.

ionic str.	charge
0.01	0.00009
0.1	0.0001
1	0.00017



Use of Tombacz fit to extrapolate to WIPP ionic strength

0.016	9.13E-05	
6	0.00057	6.244522



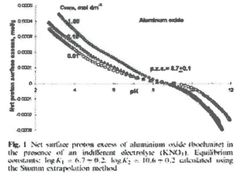


Fig. 1 Net surface proton excess of aluminium oxide (boehmite) in the presence of an indifferent electrolyte (KNO_3). Equilibrium constants: $\log K_1 = 6.7 \pm 0.2$, $\log K_2 = 10.6 \pm 0.2$ calculated using the Stumm extrapolation method

Information Only

Converts the % microbe sorbed at pH ~ 6 from Yee et al. (2000) figures 2 and 7 to Kd's

% sorbed	kd [ml/g]	(co-c)/c
30	42.9	
62	163.2	
42	72.4	
15	17.6	21
31	44.9	52

c = final microbe concentration
co = initial microbe concentration
(co-c)/c = the sorption lowering of repository microbe levels

REFERENCES

Domski, P. S. 2023. Prediction of Baseline Actinide Solubilities for the Replacement Panels Planned Change Request (RPPCR) Performance Assessment. ERMS579503.

Yee, Nathan, Jeremy B. Fein, and Christopher J. Daughney. "Experimental study of the pH, ionic strength, and reversibility behavior of bacteria–mineral adsorption." Geochimica et Cosmochimica Acta 64, no. 4 (2000): 609-617.

Calculates g/ml of Mg[OH]2, or MgO, in the Disposal Area

1.35E+09	moles MgO
6.75E+08	moles Mg[OH]2 available (half, Domski, 2023)
3.94E+10	g Mg[OH]2
1.164E+00	g/ml Mg[OH]2
1.77E-03	sites/l

1.35E+09	moles MgO
6.75E+08	moles MgO available (half)
2.72E+10	g MgO
8.05E-01	g/ml MgO

microbe-brucite surface loading calcs

4.657E-01	m2-bru/ml
5E-12	microbe-sa-side [m2]
9E+10	mgo-mic-capaci microbes/ml
0.005	m2 of mgo sites 10^9 cells/ml would occupy
0.000019	mol of mgo sites occupied

Calculated g/ml of MgO in the disposal area depends on whether it is hydrated or not because of the molecular weight difference. Both calculations are done above. Mg[OH]2 was used to calculate microbe sorption in the document.

Information Only

NOT USED IN DOCUMENT

	repository
5.39E+07	fe-kg-pkgng
6.45E+04	an-kg
8.36E+02	fe/an-mass
9.65E+08	fe-mol-pkg
2.72E+05	an-mol
3.55E+03	fe/an-mol

	cco	
300	pu-g	nas, 2020, pg 10
18120	fe-g	
1.25	pu-mol	
324.44	fe-mol	

USED IN DOCUMENT

3076379	Vol-DRZ	king[2031]	
	2.17	nacl-density	
	2.97	caso4-density	1.953
	2.25	drz-density	
	6.92185E+12	drz-mass	2.25

assume drz is 10% caso4 by wt, the rest halite. 0.1 g of caso4 = 0.297 g, 0.9 g/ml nacl = 1.953 g/ml. ergo 1 g of salado = 2.25 g/ml

Information Only